THE BELL SYSTEM TECHNICAL JOURNAL
Vol. 55, No. 7, September 1976
Printed in U.S.A.

Comparison of Equalizing and Nonequalizing Repeaters for Optical Fiber Systems

By S. D. PERSONICK

(Manuscript received October 15, 1975)

This paper compares the performances of equalizing and nonequalizing repeaters in optical fiber systems in the presence of delay distortion leading to intersymbol interference on the received optical pulse stream. Curves of receiver sensitivity loss vs delay distortion are computed for nonequalizing repeaters for various received optical pulse shapes. These results are then compared to previously published results for equalizing receivers. The results indicate that for modest delay distortion (less than 5 dB of receiver sensitivity loss) there are no significant advantages of the equalizing receiver over the nonequalizing type.

I. INTRODUCTION

This paper is concerned with the effects of intersymbol interference on the performance of equalizing and nonequalizing optical fiber system repeaters. Recent advances in the fabrication of graded-index optical fibers and improvements in laser lifetime should result in the ability to design fiber systems that are essentially loss-limited for data rates below 100 Mb/s. Nevertheless, it is interesting to study the effects of small amounts of intersymbol interference due to fiber delay distortion on the performance of optical fiber system repeaters.* Repeaters which can accommodate small amounts of intersymbol interference increase the yield of usable fibers in real cables where the index gradings are not ideal.

In a previous paper,[1] the effects of intersymbol interference on equalizing repeaters were studied. Such repeaters compensate for the fiber delay distortion (pulse spreading) by incorporating a high-frequency rollup filter in their linear channels. This rollup results in an enhancement of the receiver noise. Using the results of that paper, curves can be plotted of receiver sensitivity loss vs the spreading of the received optical pulses.

* Throughout this paper we shall assume that optical power pulses that overlap at the receiver add linearly, as justified in Ref. 3.

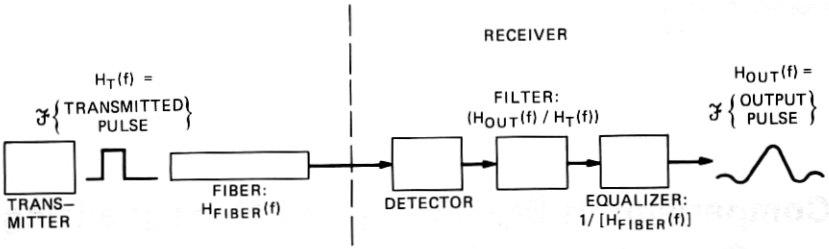

Fig. 1—Equalizing receiver.

In this paper, we shall present similar curves for nonequalizing repeaters. In such repeaters, pulse spreading results in an uncompensated closing of the receiver output "eye", leading to a sensitivity loss. Nonequalizing receivers do not require a knowledge of the

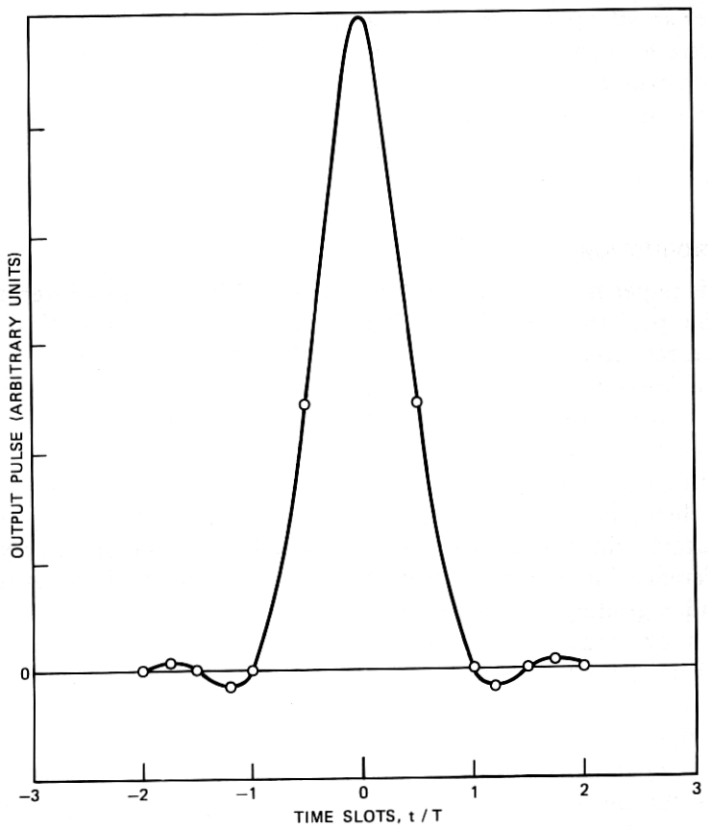

Fig. 2(a)—Ideal output pulse; $V_{out}(t)$, $T = 1.28$.

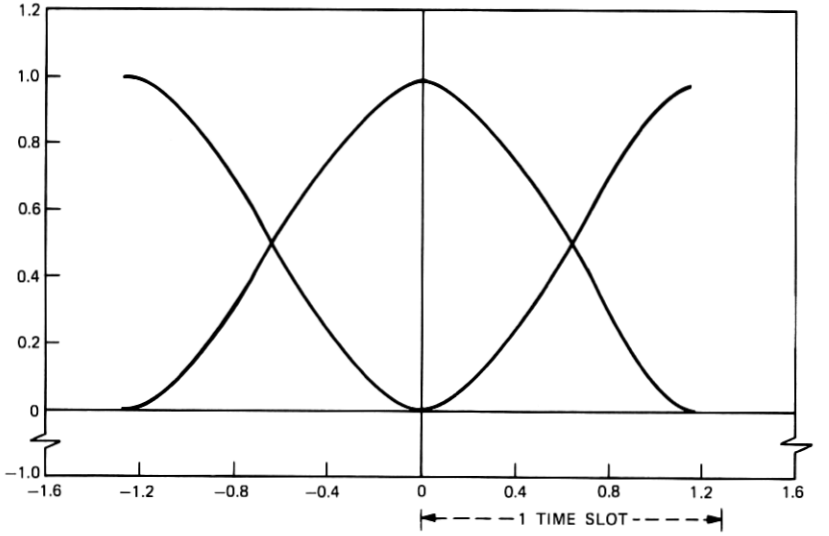

Fig. 2(b)—Ideal eye diagram; $V_{out}(t)$, $T = 1.28$.

received pulse shape. This is particularly important in systems using graded-index fibers, where residual pulse spreading, due to grading errors, can lead to unpredictable received pulse shapes.

Numerical results indicate that there is no significant advantage in equalizing over nonequalizing repeaters for sensitivity losses below 5 dB. There is no drastic deterioration in performance of the nonequalizing repeater compared to the equalizing type. As a consequence, the importance of hypothetical receivers that estimate the received pulse shape in order to adjust adaptive equalizers is considerably diminished.

II. THERMAL-NOISE-LIMITED SYSTEMS

This paper is concerned primarily with thermal-noise-limited systems. This restriction drastically simplifies the analysis compared to systems limited by randomly multiplied signal-dependent shot noise. We shall briefly discuss shot-noise-limited systems in Section III.

2.1 Equalizing receivers

An equalizing receiver is shown in Fig. 1. Observe that the output pulse shape $V_{out}(t)$ is independent of the fiber baseband frequency response $H_{fiber}(f)$. We assume that we have chosen $V_{out}(t)$ from the raised cosine family[1,2] with parameter $\beta = 1$. Figure 2 shows pictures of $V_{out}(t)$ and its associated "eye diagram." (The eye diagram is defined in the Appendix.)

The rms noise at the receiver output is dependent upon the fiber baseband frequency response (through the equalization) and the type of amplifier being used. If we normalize the eye opening to unity, we obtain an expression for the required optical power at the receiver input to achieve a 10^{-9} error rate of the following form[1]:

$$P_{\text{optical required}} = \frac{12h\Omega}{\eta} Z^{\frac{1}{2}}, \tag{1}$$

where

$\frac{h\Omega}{\eta}$ = photon energy/detector quantum efficiency

Z = normalized mean-square receiver output noise.[1]

In eq. (1), Z is an increasing function of the required equalization and is written in the following form:

$$Z = \gamma_1^2 \int_0^B |F_R(f)|^2/|H_{\text{fiber}}(f)|^2 df + \gamma_2^2 \int_0^B |F_R(f)|^2 f^2/|H_{\text{fiber}}(f)|^2 df, \tag{2}$$

where $F_R(f)$ depends upon the desired receiver output pulse and the transmitted pulse and is typically close to unity in value,

B = bit rate

γ_1, γ_2 = constants depending upon the amplifier being used.

In eq. (2), if the term involving γ_1 dominates, we have a low-impedance front end. If the term involving γ_2 dominates, we have a high-impedance front end.

Using eq. (2), we can calculate curves of the increase in required optical power (sensitivity loss) as a function of the fiber delay distortion.

2.2 *Nonequalizing receivers*

A nonequalizing receiver is shown in Fig. 3. In this receiver, the output pulse shape depends upon the baseband frequency response,

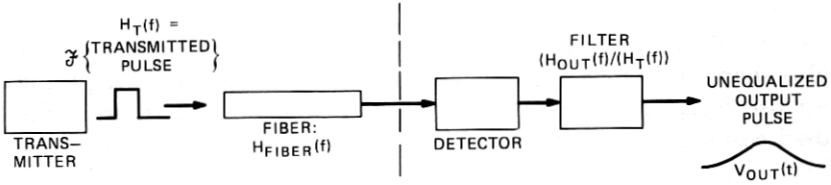

Fig. 3—Nonequalizing receiver.

but the rms noise, $Z^{\frac{1}{2}}$, does not. To calculate the receiver sensitivity, we must know the eye opening at the sampling time. We shall assume that in the absence of delay distortion in the fiber, $H_{\text{fiber}}(f) = 1$, the receiver output pulse is a raised cosine $\beta = 1$ pulse, as shown in Fig. 2. The output pulse and eye pattern resulting after delay distortion is included can be calculated in a straightforward manner. The required power to achieve a 10^{-9} error rate is given by

$$P_{\text{optical required}} = 12 \frac{h\Omega}{\eta} (\theta)^{-1} (Z_1)^{\frac{1}{2}}, \tag{3}$$

where

θ = eye opening at the sampling time ($\theta = 1$ corresponds to a completely open eye)

Z_1 = the value of mean squared thermal noise Z when there is no fiber delay distortion, i.e., Z of equation (2) with $H_{\text{fiber}}(f) = 1$.

2.3 Examples

Having defined the equalizing and nonequalizing receivers, we can now present computational results for the effects of fiber delay distortion. To make such calculations, we must specify the shape of the fiber impulse response $h_{\text{fiber}}(t)$, which is the Fourier transform of the fiber frequency response $H_{\text{fiber}}(f)$. In the examples below, we shall consider a variety of impulse response shapes.

2.3.1 Gaussian-shaped impulse response

In the absence of detailed knowledge of the fiber impulse response, we can begin by assuming a gaussian shape. Such a shape is appropriate for long fibers with mode mixing, and is given by the expression

$$h_{\text{fiber}}(t) = \exp - [\{(t/T)/(\sigma/T)\}^2/2], \tag{4}$$

where t/T is the time variable normalized to the units of time slots, and σ/T is the "rms width" of the impulse response in time slots.

Figure 4 shows curves of the deterioration of the receiver sensitivity as a function of σ/T. Curves are given for a nonequalizing receiver, a high-impedance equalizing receiver, and a low-impedance equalizing receiver. All curves are normalized to zero sensitivity loss for $\sigma/T = 0$ (sensitivity loss is the increase in required optical power in dB to maintain a fixed error rate). The curves do not show the relative performances of high- and low-impedance receivers but only the added effects of delay distortion. Figures 5 through 8 show receiver output eye diagrams and pulse shapes for $\sigma/T = 0.35$ and $\sigma/T = 0.55$ and a nonequalizing receiver.

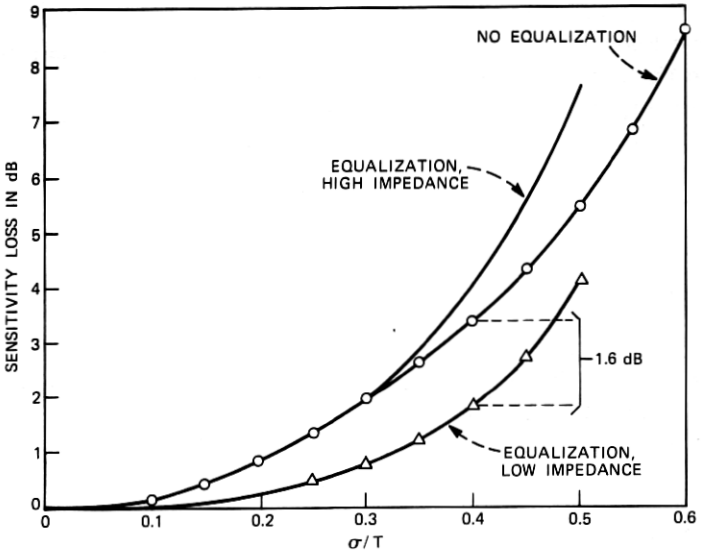

Fig. 4—Sensitivity losses vs σ/T for a gaussian impulse response, thermal noise limited.

In this example, we see that the nonequalizing receiver may be better or worse than the equalizing types depending upon the front-end design. (The optimal receiver would be some partial equalization

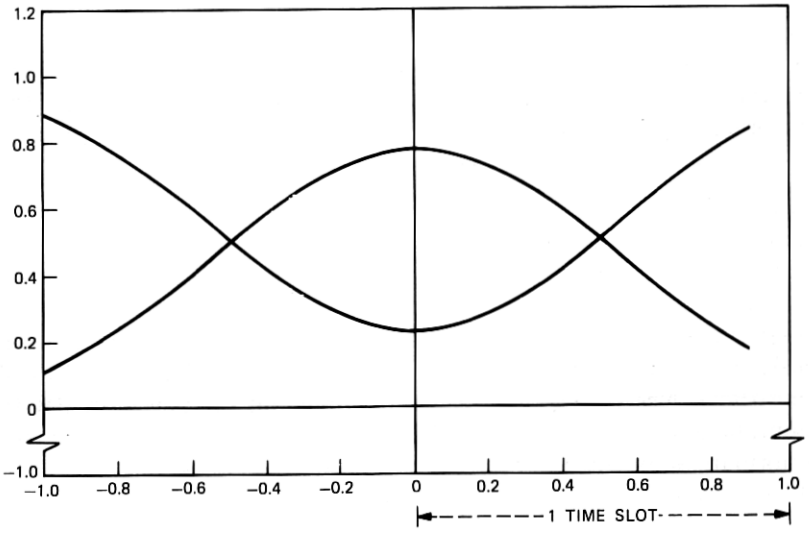

Fig. 5—Eye diagram for gaussian impulse response; $\sigma/T = 0.35$.

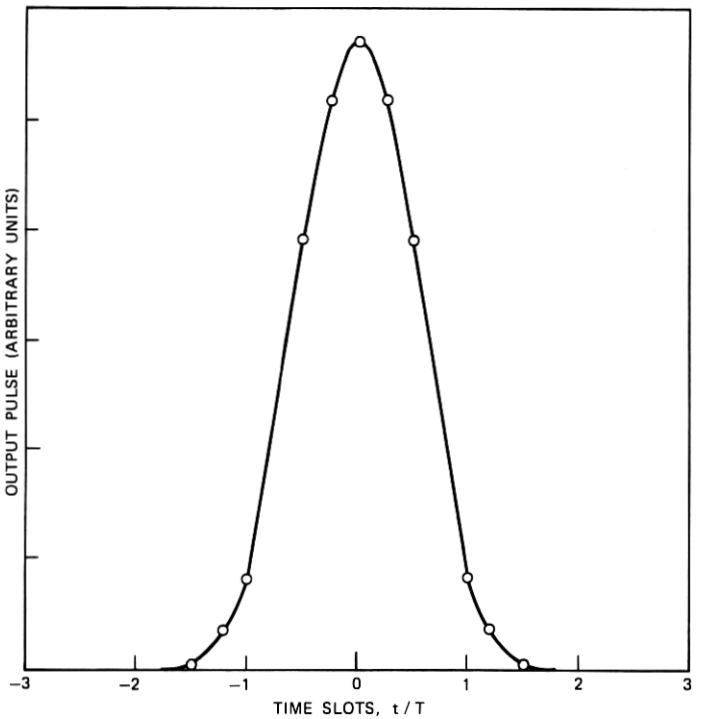

Fig. 6—Receiver output pulse for gaussian impulse response; $\sigma/T = 0.35$.

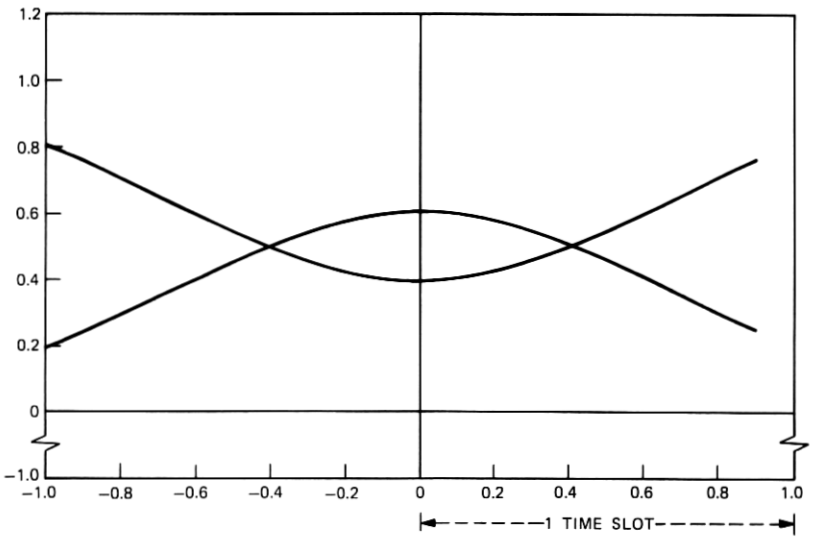

Fig. 7—Eye diagram for gaussian impulse response; $\sigma/T = 0.55$.

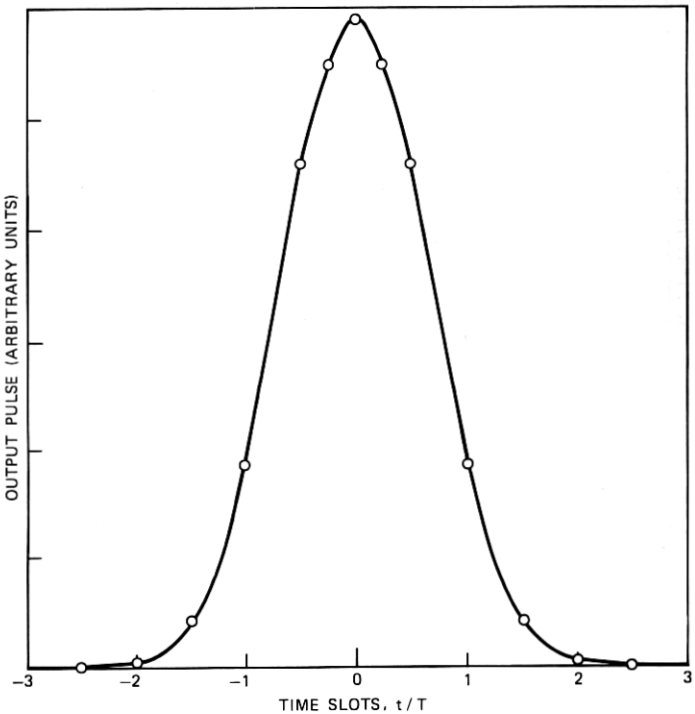

Fig. 8—Receiver output pulse for gaussian impulse response; $\sigma/T = 0.55$.

compromise between noise enhancement and intersymbol interference reduction.) The nonequalizing receiver does not deteriorate in performance at a significantly faster rate than the equalizing receiver.

2.3.2 Skew-shaped experimental pulse

Figure 9 shows a pulse response measured on an actual fiber. The fiber was 740 meters long. This pulse has an rms width $\sigma = 0.77$ ns. If we vary the bit interval T, we can calculate the receiver sensitivity loss for equalizing and nonequalizing receivers. The results are shown in Fig. 10. Figures 11 and 12 show the receiver output eye diagrams for $\sigma/T = 0.24$ and $\sigma/T = 0.6$. In Fig. 10, it is assumed that the nonequalizing receiver decision circuit samples the receiver output signal at the peak eye opening. This assumption is subject to further investigation concerning the design of timing recovery circuits.

We can propose a receiver which equalizes only the phase of the fiber baseband frequency response, leaving the amplitude rolloff uncompensated. Figure 13 shows the receiver sensitivity loss of such a phase-equalizing receiver vs σ/T. Also shown are the curves given in

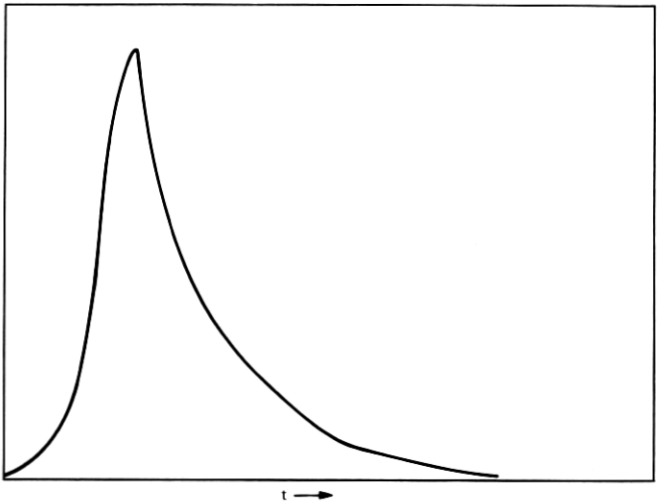

Fig. 9—Impulse response of borosilicate fiber 740 meters long.

Fig. 10. We note that the phase-equalizing receiver has no significant benefit over the nonequalizing receiver, except that sampling at the peak of the eye opening may be easier. Figure 14 shows the receiver output eye diagram for $\sigma/T = 0.6$ for the phase-equalizing receiver. This can be compared to Fig. 12.

2.3.3 Gaussian pulses on a pedestal

In fibers with graded indices, it is sometimes observed that the impulse response can be divided into two parts: (*i*) a narrow part

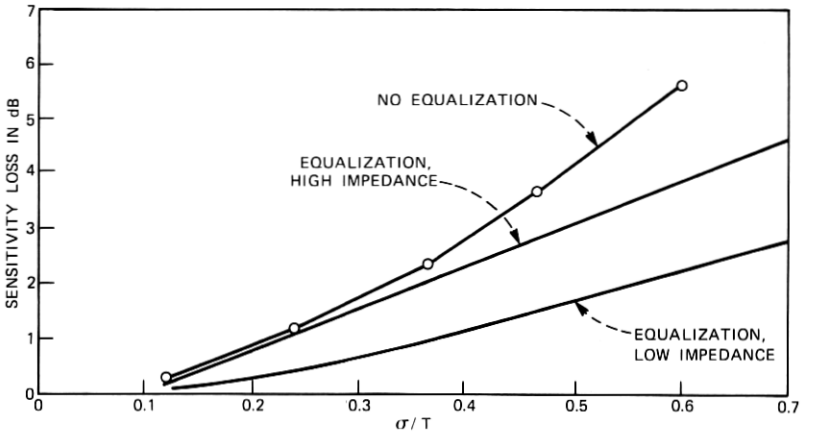

Fig. 10—Sensitivity losses vs σ/T for borosilicate fiber.

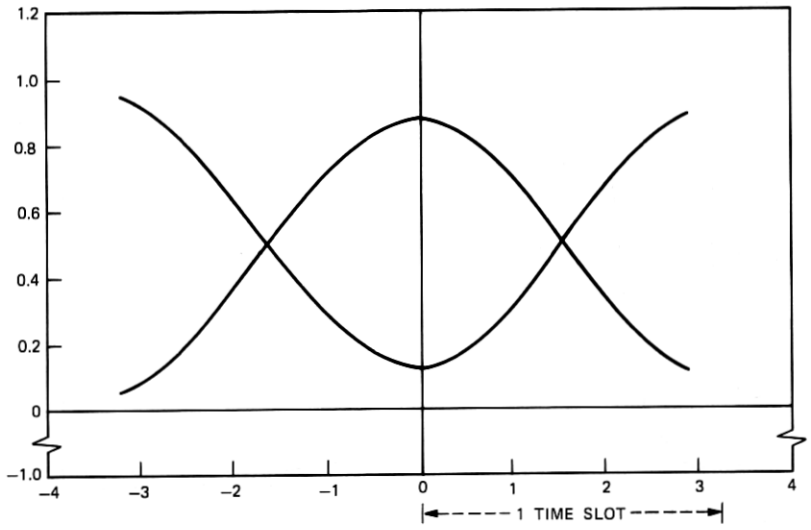

Fig. 11—Eye diagram for borosilicate fiber; $\sigma/T = 0.24$.

containing (hopefully) most of the energy and (*ii*) a wider part (tail) corresponding to high-order modes with long delays, or cladding modes coupled to the core modes. To simulate the effect of such a fiber impulse response on the system, we model it as the sum of a gaussian-

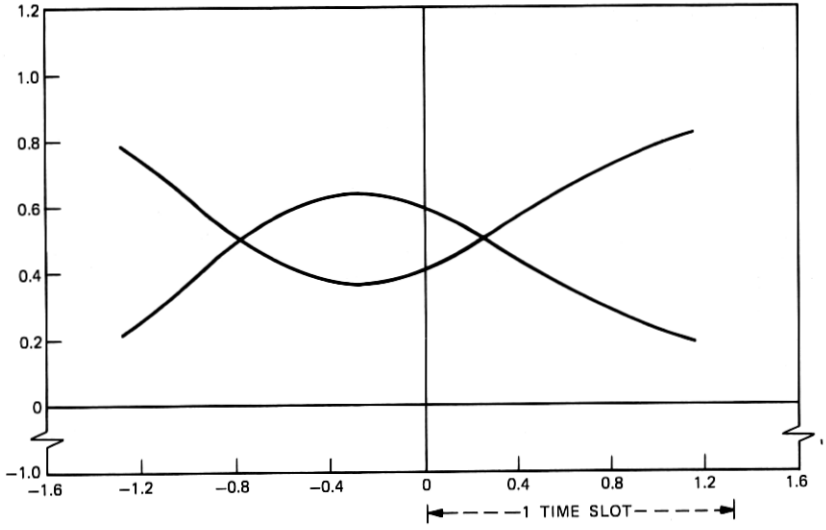

Fig. 12—Eye diagram for borosilicate fiber 740 meters long; $\sigma/T = 0.60$.

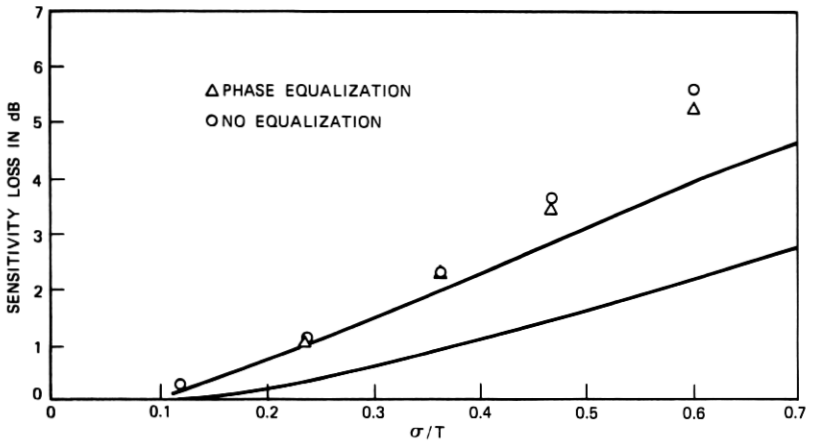

Fig. 13—Sensitivity losses vs σ/T for borosilicate fiber (includes phase equalization).

shaped pulse of area $(1 - \Delta)$ and rms width σ and a rectangular pulse of area Δ and full width W. An example is shown in Fig. 15.

Because of the uncertainty in the values of Δ, σ/T, and W/σ, which will be encountered in practice, we shall consider two cases:

Case 1: $W/\sigma = 6.4$, $\sigma/T = 0.5$, and $0 \leqq \Delta \leqq 0.2$.
Case 2: $W/\sigma = 12.8$, $\sigma/T = 0.25$, $0 \leqq \Delta \leqq 0.34$.

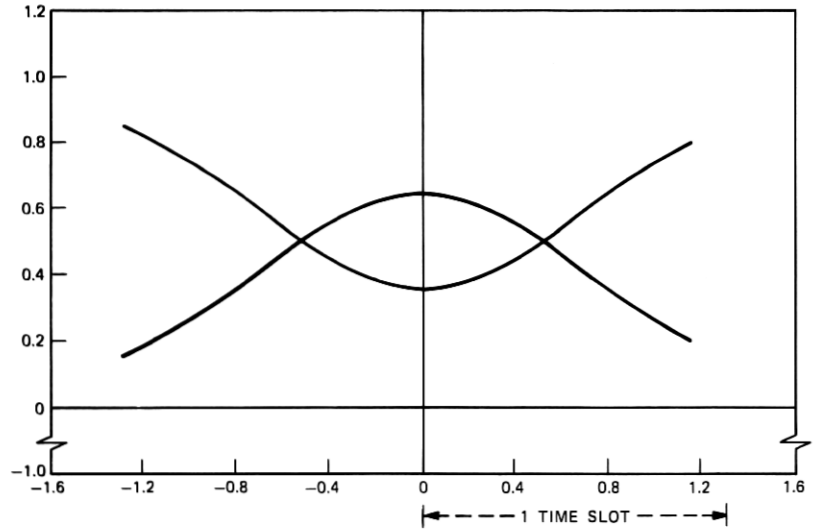

Fig. 14—Eye diagram after phase equalization for borosilicate fiber 740 meters long; $\sigma/T = 0.60$.

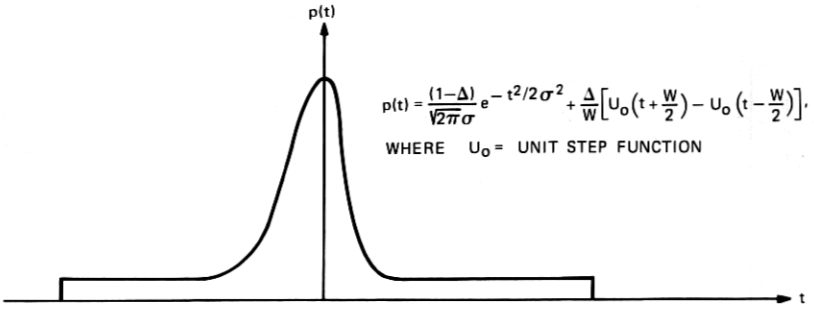

Fig. 15—Gaussian pulse on a pedestal.

Figures 16 and 17 show calculations of receiver sensitivity loss (relative to a very-narrow-shaped fiber impulse response) as a function of Δ for cases 1 and 2, respectively, and for different receivers. Also shown are curves of 10 log $[1/(1 - \Delta)]$ which correspond to the loss of total pulse energy to the pulse tail. We observe that tails affect the nonequalizing receiver more than the equalizing receiver. However, more calculations must be made to understand fully the effects of tails and how to combat those effects. Before these calculations can be made, more data on the impulse response of real fibers are needed.

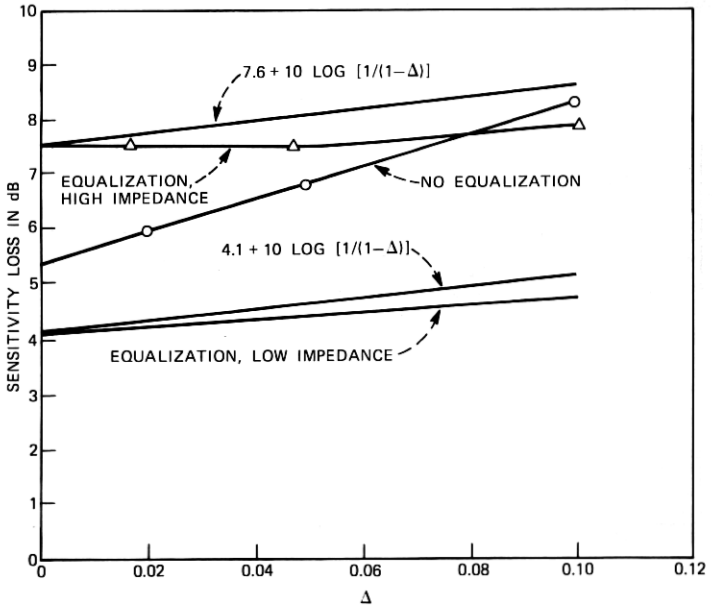

Fig. 16—Receiver sensitivity loss for Case 1: $\sigma/T = 0.5$ and $W/\sigma = 6.4$.

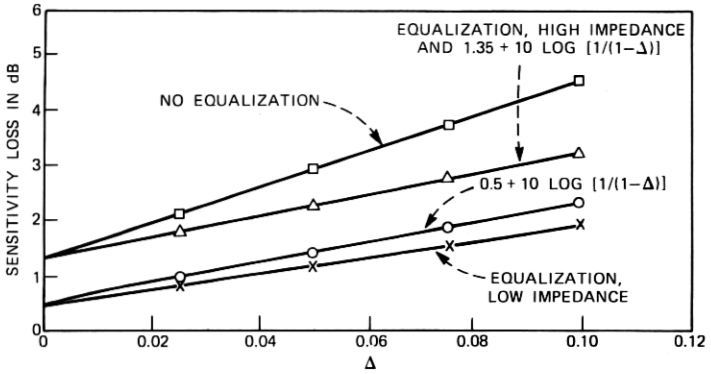

Fig. 17—Receiver sensitivity loss for Case 2: $\sigma/T = 0.25$ and $W/\sigma = 12.8$.

III. SHOT-NOISE-LIMITED SYSTEMS (AVALANCHE GAIN)

The extension of the previous results to shot-noise-limited systems requires one to take into account the signal dependence of shot noise. A rough approximation suitable for comparing nonequalizing and equalizing receivers in the following. For equalizing receivers, we can use the techniques described in Ref. 1 to calculate receiver performance degradation with increasing fiber delay distortion. Nonequalizing

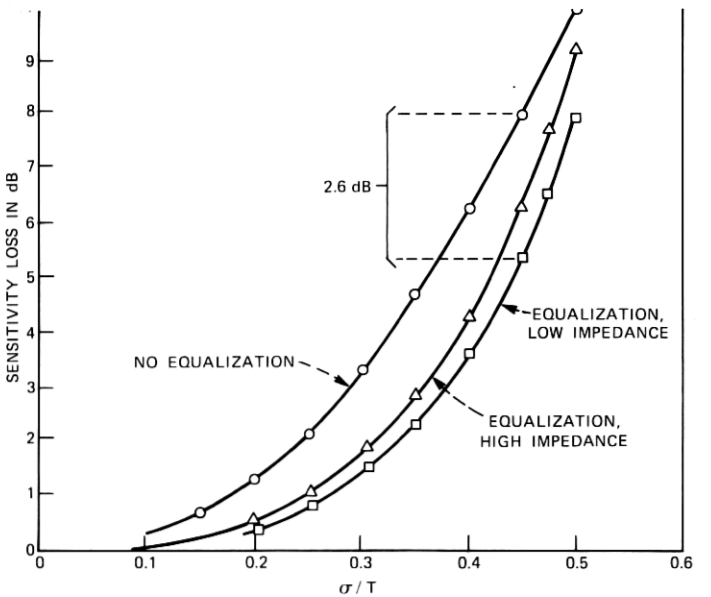

Fig. 18—Sensitivity losses vs σ/T for a gaussian impulse response, shot noise limited.

receivers can be studied by assuming that the shot noise at the receiver output is proportional to the average optical power falling on the detector, but is only weakly dependent upon the shape of the received pulses. In that case, the required received optical power increases approximately as $-50/6$ log (eye opening).[1] This can be compared to the thermal-noise-limited receiver where the required optical power increases as $-30/6$ log (eye opening).

An example of a receiver with avalanche gain is shown in Fig. 18. The figure shows a plot of receiver sensitivity loss vs σ/T for a gaussian fiber impulse response and for equalizing and nonequalizing receivers.

IV. ACKNOWLEDGMENT

The author gratefully acknowledges the work of Diane Vitello in writing programs to perform many of the above calculations.

APPENDIX

Receiver Output Eye

The output of the optical fiber receiver consists of a sequence of pulses plus noise:

$$V_{\text{out}}(t) = \sum_{k=-\infty}^{\infty} a_k h_{\text{out}}(t - kT) + n(t), \tag{5}$$

where

a_k = 0 or 1 represents the information
T = pulse spacing
$n(t)$ = noise.

In general, these pulses overlap, a characteristic which is referred to as intersymbol interference. Once every T seconds, the output is sampled (observed) to decide whether or not a pulse is present ($a_k = 1$ or $a_k = 0$). In the absence of intersymbol interference, the ability to make this decision is limited by the noise. However, due to intersymbol interference, the receiver output at the sampling time can be smaller or larger than it would be if only one pulse were present. Pessimistically, we can calculate the smallest value that $V_{\text{out}}(t)$ can assume given that the pulse we are looking for is on ($a_k = 1$), and we can also calculate the largest value that $V_{\text{out}}(t)$ can assume given that the pulse we are looking for is off ($a_k = 0$); h_{out} both of these neglect noise $n(t)$.

$$\begin{aligned} V_{\text{min on}}(t) &= h_{\text{out}}(t - kT) + \sum_{k' \neq k} [\text{min of } h_{\text{out}}(t - k'T) \text{ and } 0] \\ V_{\text{max off}}(t) &= \sum_{k' \neq k} [\text{max of } h_{\text{out}}(t - k'T) \text{ and } 0]. \end{aligned} \tag{6}$$

The "eye diagram" is a plot of $V_{\text{min on}}(t)$ and $V_{\text{max off}}(t)$ on the same abscissa (see Figs. 5 and 6). The maximum difference between the upper and lower curves (before they cross) is called the eye opening. This maximum difference occurs at a point in time where the best chance to distinguish between "pulse present" and "pulse absent" exists. The ratio of this peak eye opening to the peak height of an isolated pulse represents a loss in noise immunity and is called the fractional eye opening.

REFERENCES

1. S. D. Personick, "Receiver Design for Digital Fiber Optic Communications Systems," B.S.T.J., *52*, No. 6 (July-August 1973), pp. 843–886.
2. R. Lucky, J. Salz, and E. J. Weldon, *Principles of Data Communications*, New York: McGraw–Hill, 1968.
3. S. D. Personick, "Baseband Linearity and Equalization in Fiber Optic Digital Communication Systems," B.S.T.J., *52*, No. 7 (September 1973), pp. 1175–1194.